Research Square

Preprints are preliminary reports that have not undergone peer review.
They should not be considered conclusive, used to inform clinical practice,
or referenced by the media as validated information.

Theoretical Research on Tetrazine-Based Nitrogen-Chain Energetic Materials: Balancing Detonation Performance and Sensitivity via Structural Regulation

Qian Zhang
Huanggang Normal University
Xiao-Nan He
Huanggang Normal University
Han-Jie Ni
Huanggang Normal University
Jia-Nan Li
Huanggang Normal University
Lan-Ying Xu
Huanggang Normal University
Yan Huang
huangychem@hgnu.edu.cn
Huanggang Normal University
Tao Long
Huanggang Normal University

Research Article

Keywords: Density functional theory, Tetrazine-Based, Nitrogen-chain energetic materials, Thermodynamic stability

Posted Date: September 24th, 2026

DOI: https://doi.org/10.21203/rs.3.rs-10889963/v1

License: This work is licensed under a Creative Commons Attribution 4.0 International License.
Read Full License

Additional Declarations: No competing interests reported.

Version of Record: A version of this preprint was published at Journal of Molecular Modeling on November 14th, 2026. See the published version at https://doi.org/10.1007/s00894-026-07046-2.

Theoretical Research on Tetrazine-Based Nitrogen-Chain Energetic Materials: Balancing Detonation Performance and Sensitivity *via* Structural Regulation

Qian Zhang, *Xiao-Nan He*, *Han-Jie Ni*, *Jia-Nan Li*, *Lan-Ying Xu*, *Yan Huang** *and Tao Long**

School of Chemistry and Chemical Engineering Huanggang Normal University, Huanggang 438000, China

Author Information

Ph.D Qian Zhang, E-mail: zhangqian2024@hgnu.edu.cn, Tel +86 1885118942,

ORCID id: 0009-0002-4542-0407;

Ph.D Yan Huang, E-mail: huangychem@hgnu.edu.cn, Tel +86 17551157285,

ORCID id: 0009-0003-4727-4754;

Prof. Tao Long, E-mail: 14011810@qq.com, Tel +86 15098003879;

Prof. Lan-Ying Xu, E-mail: 81666230@qq.com, Tel +86 18972720868;

Xiao-Nan He, E-mail: hhh225398@qq.com, Tel +86 19837677585;

Han-Jie Ni, E-mail: 1782150335@qq.com, Tel +86 19074692349;

Jia-Nan Li, E-mail: 1598600196@qq.com, Tel +86 15872827137.

Mailing address: Huanggang Normal University, Huanggang 438000, China

Abstract

Context Herein, we proposed a strategy using a 1,2,3,4-tetrazine ring as the molecular skeleton to construct nitrogen-chain frameworks. A series of tetrazine-based molecules (Series **I**-**IV**) were designed and investigated *via* DFT calculations. The tetrazine-based scaffold retained high nitrogen content and density while offering enhanced thermodynamic stability over triazole-based analogues. Over half of the designed molecules displayed densities higher than 1.80 g/cm^3 and several derivatives even exceeded 1.90 g/cm^3 (1.902-1.965 g/cm^3). Predicted detonation velocities (8.926-11.32 km/s) and pressures (33.94-59.18 GPa) surpassed those of triazole-based analogues and HOF (948.8-1951 kJ/mol) were markedly higher. This work established a theoretical framework that may guide the rational design and experimental synthesis of next-generation insensitive high-energy materials.

Method Geometry optimizations and frequency analyses were carried out with Gaussian 09 using the B3PW91/6-311+G(d,p) and M06-2X/6-311+G(d,p) method, respectively. Isodesmic reactions were

employed to obtain heat of formation (HOF), while Multiwfn 3.8_dev software was used for calculations of HOMO-LUMO energy gaps (ΔE), electrostatic potentials (ESP) and other relevant descriptors. Weak intermolecular interactions in the dimers were visualized *via* VMD 1.9.3 program.

Keywords: Density functional theory, Tetrazine-Based, Nitrogen-chain energetic materials, Thermodynamic stability

Introduction

Nitrogen-rich energetic materials were promising candidates for high-performance explosives and propellants, featuring high nitrogen content, high formation enthalpies and clean decomposition products [1,2]. The 5,5'-bis(trinitromethyl)-3,3'-azo-1,2,4-triazole hemihydrate, synthesized by Shreeve and colleagues, was reported to exhibit detonation performance (ρ = 1.83 g/cm^3, HOF = 555.1 kJ/mol, P = 36.65 GPa, D = 8.964 km/s) comparable to that of RDX (ρ = 1.82 g/cm^3, HOF = 92.6 kJ/mol, P = 35.17 GPa, D = 8.997 km/s) [3]. However, its impact sensitivity (IS = 1.5 J) was significantly lower than that of RDX (IS = 7.4 J), which severely restricted its practical application.

Fully nitrogen-chained frameworks, which consisted of contiguous N-N or N=N bonds, offered higher thermodynamic stability [4,5]. The 1,1'-azobis-1,2,3-triazole showed a HOF of 962 kJ/mol and an h_{50} value of 16.6 cm, but it remained slightly more sensitive than RDX (h_{50} = 28 cm) and exhibited a relatively low density of only 1.64 g/cm^3 (**Fig. 1a**) [6]. The introduction of NO_2-groups as energetic substituents, as in 1,2-bis(3-nitro-1H-1,2,4-triazol-1-yl)diazene, increased the density to 1.80 g/cm^3 but significantly decreased the HOF to 719 kJ/mol [7]. Parrish and colleagues synthesized 2,9-dinitrobis([1,2,4]triazolo)-[1,5-d:5',1'-f][1,2,3,4]tetrazine *via* construction of an azo-coupled fused tricyclic 1,2,3,4-tetrazine framework [8]. Compared with 1,2-bis(3-nitro-1H-1,2,4-triazol-1-yl)diazene, this energetic material showed improved density (1.91 g/cm^3) and HOF (787 kJ/mol).

In contrast to the inherently unstable zolene-based and azo-bridged frameworks, tetrazine-based systems offered significantly enhanced thermodynamic stability while maintaining high nitrogen content and density [9]. As illustrated in **Fig. 1b**, the energetic material **BATT** [10] and **DAAT** [11] exhibited substantially higher HOF than 1,2-bis(3-nitro-1H-1,2,4-triazol-1-yl)diazene, despite having comparable densities. Furthermore, functionalization of **DAAT** with $C(NO_2)_3$-groups was shown to increase both density (to 1.83 g/cm^3) and HOF (to 1184 kJ/mol) [11]. These findings suggested that tetrazine-based energetic compounds had the potential to balance detonation performance with thermodynamic stability.

In this work, we used the 1,2,3,4-tetrazine ring as molecular scaffold to design a series of energetic molecules with nitrogen-chained frameworks (**Fig. 1c**). Systematic DFT calculations were then performed to screen and evaluate potential candidates with promising detonation performance and thermodynamic stability.

Computational Methods

All molecular calculations were carried out with the Gaussian 09 program package [12]. Previous studies have demonstrated that the B3PW91 functional was well suited for geometry optimization of nitro-containing molecules [13], whereas the M06-2X functional provided more accurate thermodynamic data [14] and the ωB97X-D functional exhibited better performance in describing weak intermolecular interactions [15]. Accordingly, geometry optimizations of all designed molecules were carried out at the B3PW91/6-311+G(d,p) level, frequency analyses at the M06-2X/6-311+G(d,p) level and subsequent investigations of dimeric weak intermolecular interactions were performed using the ωB97X-D/def2tzvp method. The HOF, a key property of an energetic molecule that was used to assess its

potential thermodynamic stability in application, was calculated using isodesmic reactions [16]. Then the detonation performance parameters were calculated using Kamlet-Jacobs equations [17] (detonation velocity $D = 1.01(N\bar{M}^{0.5}Q^{0.5})^{0.5}(1 + 1.30\rho)$; detonation pressure $P = 1.558\rho^2 N\bar{M}^{0.5}Q^{0.5}$). The AV1245 method [18] was used to analyze the aromaticity of molecular and to characterize the configuration of LOL-pi electrons, which were realized by the Multiwfn_3.8_dev software [19, 20]. Then, the weak intermolecular interaction was presented with NCI analysis using the ωB97X-D/def2tzvp method, which was visualized by VMD 1.9.3 program [21, 22]. The AICD map was generated using pov-ray 3.7.0 software for visualization. The dimer was rapidly generated with the Molclus genmer program [23] and screened in combination with Gaussian 09 program package.

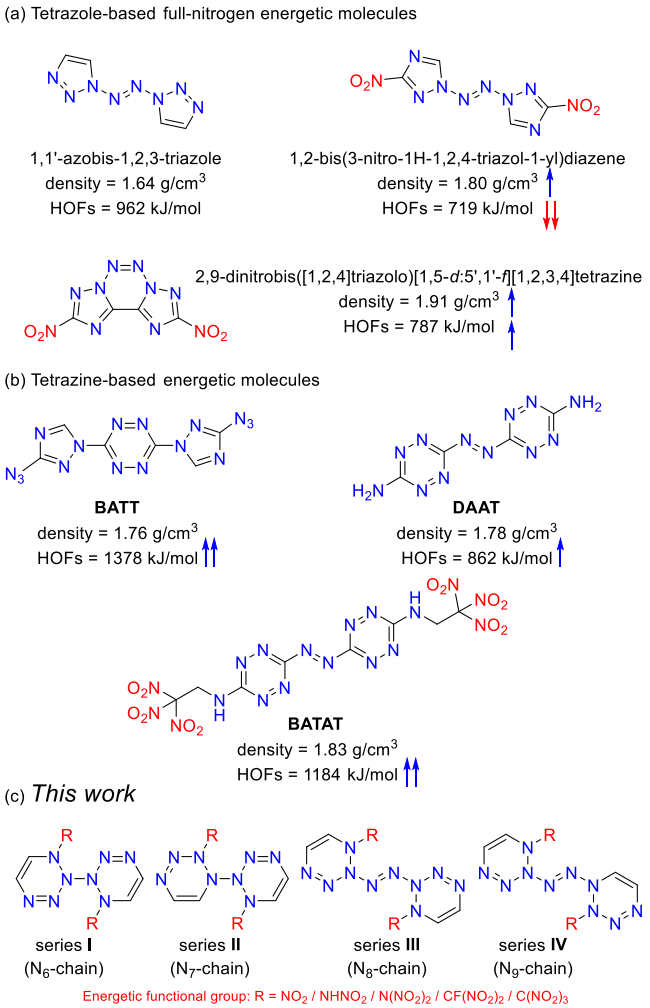


Fig. 1 (a) Tetrazole-based full-nitrogen energetic molecules, (b) Tetrazine-based energetic molecules, (c) The design of energetic materials structures with 1,2,3,4-tetrazine ring as the molecular framework.

Results and Discussion

Molecular Geometry and Stability

Employing 1,2,3,4-tetrazine ring as the fundamental molecular framework, we designed a series of nitrogen-chained molecules incorporating N_6 through N_{10} chains, achieved by modulating the relative positions of N-N single and N=N double bonds in the bridging unit (Fig. **S1**). Comparative density analysis indicated that molecules **3** (1.641 g/cm^3), **6** (1.608 g/cm^3), **12** (1.653 g/cm^3) and **15** (1.637 g/cm^3) possess higher density values (Table **S1**, calculated at M06-2X/6-311+G(d,p) level). Based on this, four new series of molecules (Series **I**-**IV**, Fig. **S2**) were constructed from their frameworks to

investigate whether molecules bearing both the 1,2,3,4-tetrazine ring and nitrogen-chains had the potential to serve as high-energy insensitive energetic materials.

Geometry optimization afforded the equilibrium structures of the designed molecules. All optimized structures exhibited good symmetry and have calculated densities exceeding 1.80 g/cm^3 (Table **S2**). Notably, eight molecules (**I-04** to **I-06**, **II-04** and **II-05**, **III-05** and **III-06**, **IV-06**) with theoretical densities exceeding 1.90 g/cm^3 (1.902-1.965 g/cm^3, **Fig. 2** and **Table 1**).

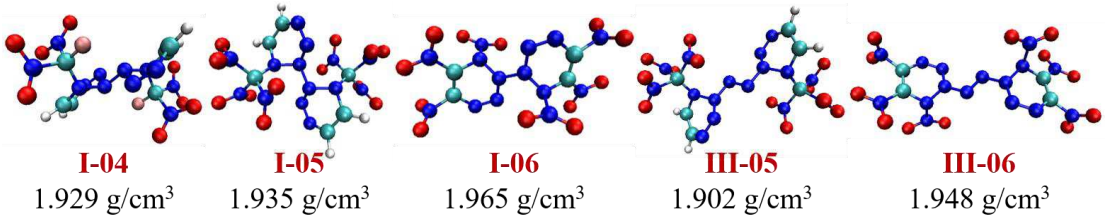


Fig. 2 Molecular optimization structure and density of designed molecule **I-04** to **06** and **III-05** to **06** at B3PW91/6-311+G(d,p) level

During geometric optimization, molecules **I-04** to **06** and **III-05** to **06** exhibited excellent structural stability. In contrast, other molecules with theoretical densities above 1.90 g/cm^3, such as **IV-06** (1.925 g/cm^3, **Table S2**), underwent ring opening of the 1,2,3,4-tetrazine ring during optimization process. Further analysis indicated that increasing the number of NO_2-groups on the 1,2,3,4-tetrazine framework significantly raised the molecular density, but also enhanced the instability of the N-NO_2 bonds, making them more prone to cleavage. This trend was reflected in the HOMO-LUMO energy gaps (ΔE). The molecule **II-06** (four NO_2-groups, 1.872 g/cm^3) had a ΔE value as 6.553 eV (Table **S3**). **I-06** and **III-06** (six NO_2-groups) exhibited lower ΔE value of 5.511 eV and 5.424 eV, respectively (**Fig. 3**).

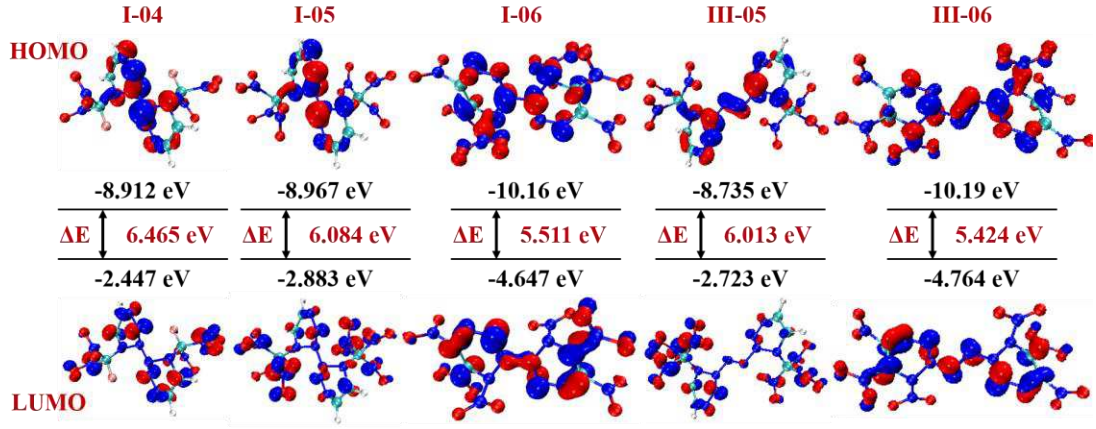


Fig. 3 HOMO and LUMO orbitals map and energy gaps of designed molecule **I-04** to **06** and **III-05** to **06** at M06-2X/6-311+G(d,p) level

Detonation Properties

A structurally similar triazole-based energetic molecule **M02** and **M03** (Table **S4**) were selected as reference to evaluate the detonation performance of the designed molecules (Table **1**). More than half of the designed molecules exhibited density values comparable to or higher than that of **M02** (1.745 g/cm^3 at the B3PW91/6-311+G(d,p) level) (**Fig. 4a**). The calculated HOF of the designed molecules, ranging from 948.8 to 1951 kJ/mol (**Fig. 4b**), were significantly superior to that of **M02** (719.2 kJ/mol). However, their predicted impact sensitivities (h_{50}) ranged from 14.62 to 48.09 cm (**Fig. 4c**). These values were generally inferior to that of **M02** (32.51 cm), but significantly superior to those of **M03** (19.75 cm). In terms of detonation performance, all designed molecules showed excellent values, with

detonation velocities of 8.926-11.32 km/s (**Fig. 4e**) and detonation pressures of 33.94-59.18 GPa (**Fig. 4f**). Compared with triazole-based nitrogen-chain energetic materials, the tetrazine-based nitrogen-chain molecules investigated here demonstrated the potential to maintain or even enhance detonation performance while simultaneously reducing sensitivity.

Table 1 Detonation properties of the designed molecules (at M06-2X/6-311+G(d,p) level)

Compd.	ρ^a	$\Delta H_f^{0\ b}$	$Q^{\ c}$	$D^{\ d}$	P^e	$T_{bp}{}^f$	$h_{50}{}^g$
I-01	1.721	1396	2119	8.973	34.75	740.7	42.07
I-02	1.694	1561	2074	8.952	34.25	876.1	43.97
I-03	1.856	1641	2100	9.780	43.21	886.0	22.71
I-04	**1.929**	948.8	2386	11.32	59.18	909.1	20.53
I-05	**1.935**	1267	1914	9.722	43.74	963.3	20.53
I-06	**1.965**	1308	2010	10.12	47.83	1001	14.62
II-01	1.732	1396	2119	9.013	35.20	737.8	42.13
II-02	1.685	1568	2080	8.926	33.94	842.7	33.73
II-03	1.860	1645	2103	9.799	43.43	868.2	25.85
II-04	**1.920**	951.9	2300	11.02	55.96	897.3	26.85
II-05	**1.932**	1276	1919	9.718	43.66	922.8	15.53
II-06	1.872	1350	2050	9.695	42.67	897.5	24.01
III-01	1.718	1720	2184	9.103	35.73	833.8	44.83
III-02	1.686	1876	2128	9.031	34.75	999.9	46.81
III-03	1.838	1951	2138	9.783	42.98	1014	31.61
III-04	1.897	1262	2404	11.17	57.11	1023	30.16
III-05	**1.902**	1573	1954	9.682	42.95	1088	20.37
III-06	**1.948**	1626	2053	10.13	47.70	1086	16.31
IV-01	1.719	1717	2182	9.104	35.75	847.5	46.04
IV-02	1.686	1882	2133	9.036	34.79	970.6	48.09
IV-03	1.810	1941	2132	9.671	41.62	1057	37.67
IV-04	1.872	1255	2400	11.06	55.57	1056	38.58
IV-05	1.881	1568	1952	9.603	41.98	1109	23.87
IV-06	**1.925**	1620	2050	10.05	46.55	1118	24.80
M02	1.745 (1.80) [7]	719.2	1459	8.373 (8.825) [7]	31.10 (33.5) [7]	922.9	32.51
M03	1.877 (1.907) [8]	787	1492	8.694 (9.4) [8]	34.68 (38) [8]	722.9	19.75

[a] density (kg/cm^3), at B3PW91/6-311+G(d,p) level
[b] solid phase heat of formation (kJ/mol);
[c] explosion heat (J/g);
[d] detonation velocity (km/s);
[e] explosion pressure (GPa);
[f] boiling point (°C);
[g] impact sensitivity (cm).

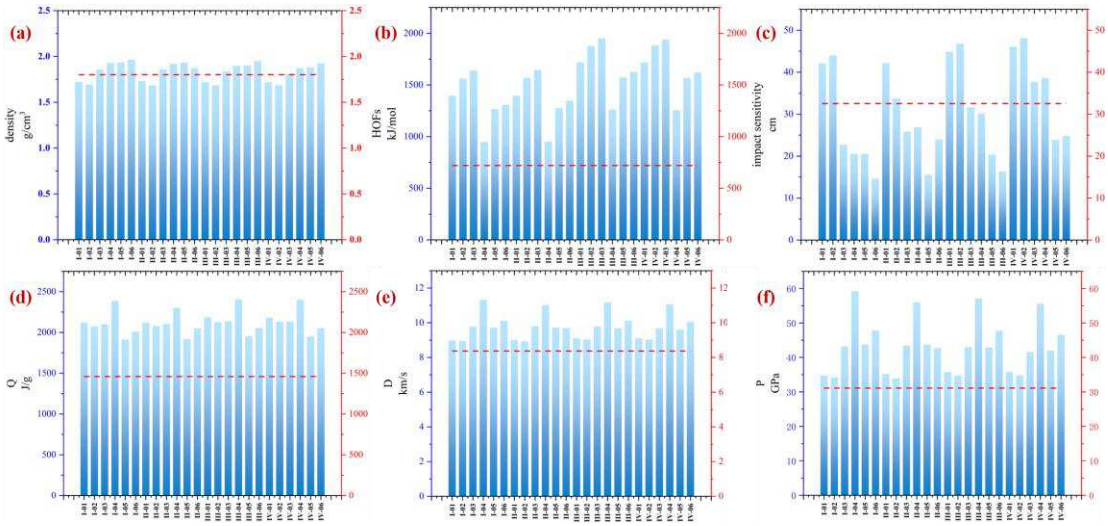


Fig. 4 Detonation properties of the designed molecules, compared with those of compound **M02** (red dotted line) at M06-2X/6-311+G(d,p) level. (**a**) Predicted density value, (**b**) predicted HOFs value, (**c**) predicted impact sensitivity (h_{50}) value, (**d**) predicted explosion heat (Q) value, (**e**) predicted detonation velocity (D) value, (**f**) predicted explosion pressure (P) value.

Electrostatic Potential and Aromatic Properties

To investigate the electrostatic potential of designed molecules, surface electrostatic potential (ESP) and LOL-pi distribution research were constructed (**Fig. 5**). The ESP analysis showed that for **I-04**, **I-05** and **III-05**, positive regions (red) were predominantly concentrated around the C=C double bonds, whereas negative regions (blue) were localized on the NO_2-groups. In contrast, for **I-06** and **III-06**, although negative potential remained on the NO_2-groups, the positive potential extended over the entire 1,2,3,4-tetrazine framework, implying more extensive electron-deficient domains. Further insight into pi-electron localization was obtained from LOL-pi density maps. The LOL-pi electrons of **I-04**, **I-05**, **III-05** and **III-06** were found to be diffusely distributed over the whole molecular skeleton, indicating appreciable π delocalization. Conversely, for **I-06**, the LOL-pi density was largely confined to the NO_2-groups, while the 1,2,3,4-tetrazine framework exhibited sparse pi-electron distribution.

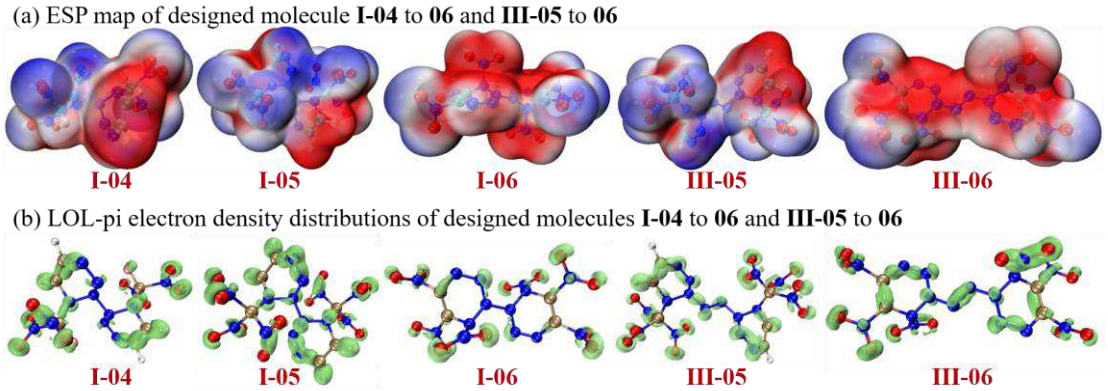


Fig. 5 Electrostatic potential (at M06-2X/6-311+G(d,p) level): (**a**) ESP map of designed molecule **I-04** to **06** and **III-05** to **06**, (**b**) LOL-pi electron density distributions of designed molecules **I-04** to **06** and **III-05** to **06**.

The magnetically induced current density maps (**Fig. S7**), generated *via* the AICD program [24], revealed that the induced ring current in the designed molecules **I-04** to **06** and **III-05** to **06** were

disordered and lacked a coherent direction, failing to exhibit the typical clockwise circulation expected for aromatic systems. Both the AICD study results and the AV1245 calculations (Table **S7**) consistently confirmed the absence of aromaticity in the designed molecules **I-04** to **I-06** and **III-05** to **III-06**.

Molecular Interactions

The ESP distribution and aromaticity analyses indicated that the designed molecules were unlikely to participate in π-π stacking interactions. Based on the distribution of pi-electron in the molecule, molecule **III-06** was selected as the research object. We systematically investigated the intermolecular noncovalent interactions within its dimer. The dimeric structure was constructed using the genmer module of the Molclus program and then fully optimized at the ωB97X-D/def2tvzp level with Gaussian 09 software. The ESP map of the optimized dimer (**Fig. 6a**) showed that the intermolecular interaction forces were dominated by repulsive electrostatic regions, ruling out favourable π-π stacking. The NCI scatter graph (**Fig. 6b**) exhibited only two distinct spikes, corresponding to H-bond (green) and steric effect (red), whereas no signature of vdW interactions was observed. The NCI RDG filling map (**Fig. 6c**) visually confirmed the spatial regions of these H-bond (green) and steric effect (red). The presence of these directional H-bond sites provided a handle for tuning interlayer cohesion without relying on π-π interactions.

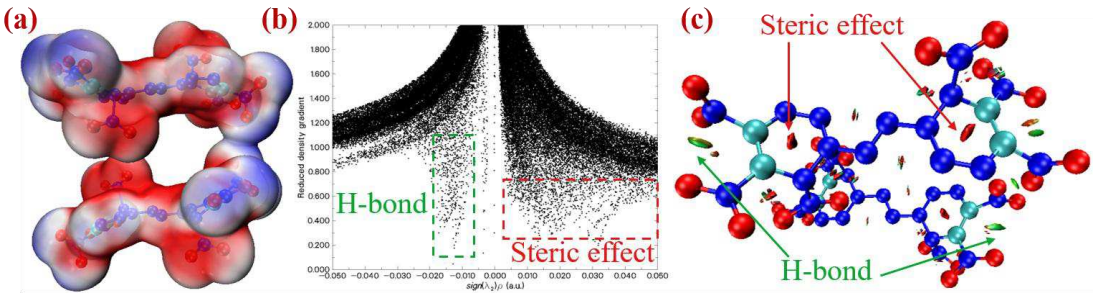


Fig. 6 Study on the weak interactions between molecule **III-06** dimer. (a) The ESP map of the optimized **III-06** dimer, (b) The NCI scatter graph of the **III-06** dimer, (c) The NCI RDG filling map of the **III-06** dimer. (at ωB97X-D/def2tvzp level)

Possible decomposition pathway

Fig. 7 illustrated the proposed decomposition pathways of molecule **I-06** (for further details, see Supporting Information **Fig. S8** and **Table S8**), with the green-highlighted pathway representing the thermodynamically most favorable route. The decomposition process proceeded in three distinct stages. In the first stage, the decomposition initiated with sequential cleavage of the two N-NO_2 bonds attached to the 1,2,3,4-tetrazine ring, with Gibbs free energy barriers (ΔG) of 8.48 kcal/mol and 5.77 kcal/mol, respectively. Subsequent scission of the N-N bridge bond (ΔG = 12.7 kcal/mol) fragmented intermediate **I-06-B** into **I-06-C**, which retained the 1,2,3,4-tetrazine ring and initiated the second stage. In the second stage, ring rupture of the 1,2,3,4-tetrazine moiety competed kinetically with further NO_2-group dissociation. The barriers for cleavage of the N(1)-N(2) and N(2)-N(3) bonds in **I-06-C** were 6.13 kcal/mol and 8.09 kcal/mol, respectively, whereas NO_2-group elimination at the 5- and 6-positions required 56.0 and 57.0 kcal/mol. Notably, cleavage of the N(1)-N(2) bond was accompanied by loss of the 6-position NO_2-group, affording intermediate **I-06-F**. From **I-06-F**, three competing routes were evaluated: 5-position NO_2-group elimination (ΔG = 13.6 kcal/mol), N(3)-N(4) bond rupture (ΔG = 21.1 kcal/mol) and C(5)-C(6) bond cleavage (ΔG = 95.2 kcal/mol). The lowest-barrier process was

5-position NO_2-group elimination, which yielded **I-06-L** and was therefore kinetically favored. In the third stage, complete fragmentation of **I-06-L** to two molecules of C≡N and one molecule of N≡N proceeded with a barrier of 56.4 kcal/mol, making this final step the rate-determining step of the overall decomposition.

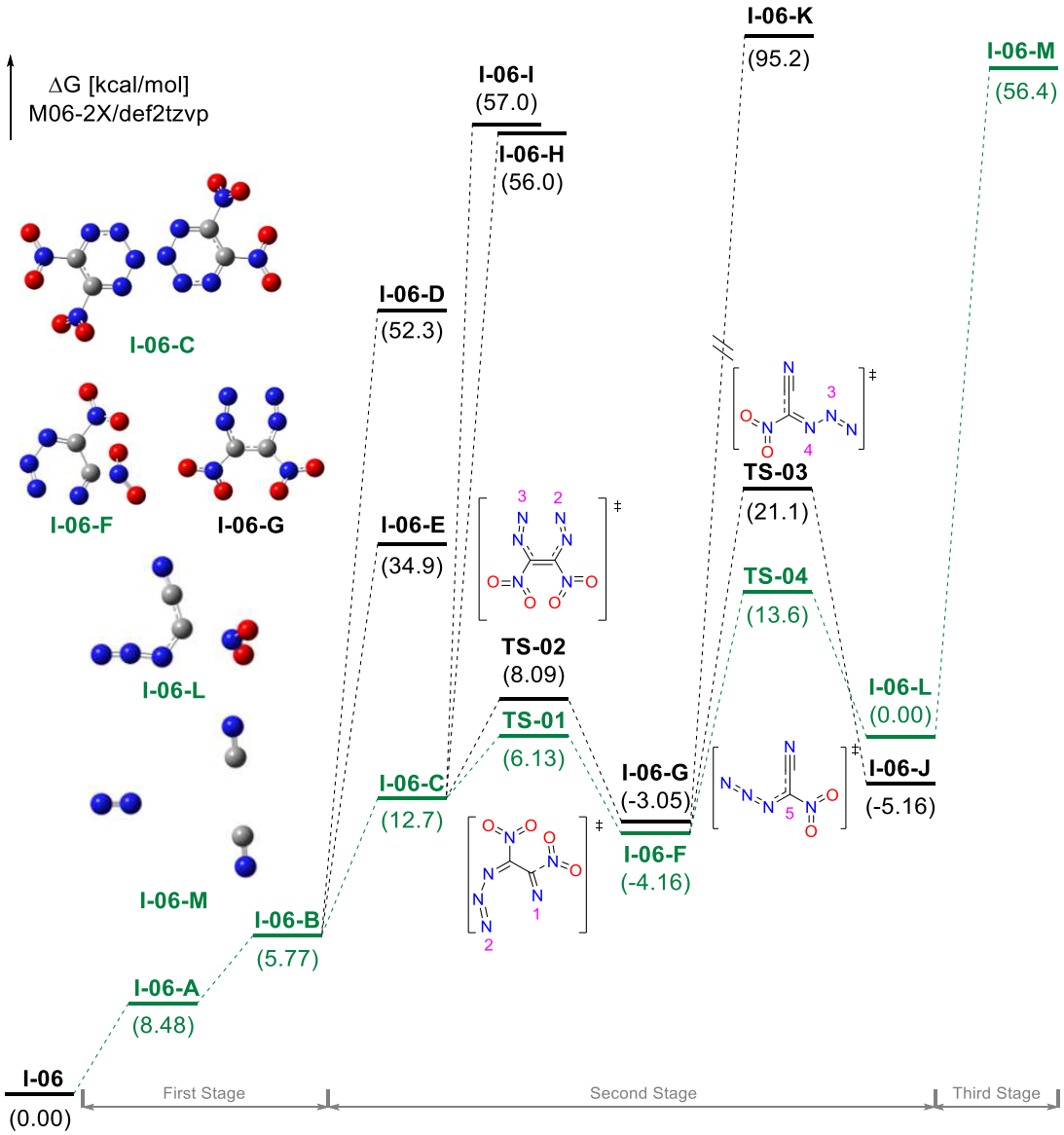


Fig. 7 Possible decomposition pathway of molecule **I-06** (at M06-2X/def2tzvp level)

Conclusions

In this study, a series of tetrazine-based nitrogen-chain energetic molecules (Series **I-IV**) were designed and systematically investigated using DFT calculations. Compared with triazole-based frameworks, the 1,2,3,4-tetrazine ring served as a more robust scaffold, combining high nitrogen content with enhanced thermodynamic stability. More than half of the designed molecules achieved densities comparable to or higher than that of similar triazole-based molecules, with markedly superior HOF (948.8-1951 kJ/mol) and outstanding predicted detonation properties (D = 8.926-11.32 km/s, P = 33.94-59.18 GPa). Further investigations into the electronic structure and weak interactions have revealed that H-bond-mediated

interlayer cohesion may offer a pathway for reducing mechanical sensitivity. In summary, the tetrazine-based nitrogen-chain scaffold demonstrated significant potential for the development of high-energy-density materials. The theoretical insights gained from this study provided a valuable foundation for guiding future experimental synthesis and the rational design of insensitive high-energy materials.

References

1. Yadav AK, Dharavath S (2025) Shaping the future of energetic materials: breakthroughs, barriers, and emerging frontiers. Chem. Commun. 61 (85): 16547-16559.
https://doi.org/10.1039/d5cc04730g

2. Li DX, Cui YR, Ruan KX, Li LJ, Zhang XF, Zhou YT, Lu M, Xu YG (2025) Research Progress on the Synthesis of Tetrazole-based Nitrogen-rich Energetic Compounds. Chinese Journal of Energetic Materials 33(5): 523-553.
https://doi.org/10.11943/CJEM2025071

3. Thottempudi V, Gao HX, Shreeve JM (2011) Trinitromethyl-Substituted 5-Nitro- or 3-Azo-1,2,4-triazoles: Synthesis, Characterization, and Energetic Properties. J. Am. Chem. Soc. 133: 6464-6471.
https://doi.org/10.1021/ja2013455

4. O'Sullivan OT, Zdilla MJ (2020) Properties and Promise of Catenated Nitrogen Systems As High-Energy-Density Materials. Chem. Rev. 120(12): 5682-5744.
https://doi.org/10.1021/acs.chemrev.9b00804

5. Xu Z, Lu M (2025) Research Progress of All-nitrogen Ions and Long Nitrogen Chains Energetic Materials. Chinese Journal of Energetic Materials, 33(9): 993-1004.
https://doi.org/10.11943/CJEM2025100

6. Li YC, Qi C, Li SH, Zhang HJ, Sun CH, Yu YZ, Pang SP (2010) 1,1'-Azobis-1,2,3-triazole: A High-Nitrogen Compound with Stable N8 Structure and Photochromism. J. Am. Chem. Soc. 132: 12172-12173.
https://doi.org/10.1021/ja103525v

7. Yin P, Parrish DA, Shreeve JM (2014) *N*-Diazo-Bridged Nitroazoles: Catenated Nitrogen-Atom Chains Compatible with Nitro Functionalities. Chem. Eur. J. 20: 1-7.
https://doi.org/10.1002/chem.201402762

8. Chavez DE, Bottaro JC, Petrie M, Parrish DA (2015) Synthesis and Thermal Behavior of a Fused, Tricyclic 1,2,3,4-Tetrazine Ring System. Angew. Chem. Int. Ed. 54: 12973-12975.
https://doi.org/10.1002/anie.201506744

9. Fershtat LL (2023) Recent advances in the synthesis and performance of 1,2,4,5-tetrazine-based energetic materials. FirePhysChem 3: 78-87.
https://doi.org/10.1016/j.fpc.2022.09.005

10. Chavez DE, Gilardi RD (2009) Synthesis of 3,6-bis(3-azido-1,2,4-triazol1-yl)-1,2,4,5-tetrazine. Journal of Energetic Materials, 27(2): 110-117.
http://dx.doi.org/10.1080/07370650802405224

11. Yu GM, Yang HW, Lü CX, Cheng GB (2014) Synthesis and Characterization of Trinitroethyl Compounds Derived from Terazine. Chinese Journal of Energetic Materials 22(6): 736-740.
https://doi.org/10.11943/j. issn.1006-9941.2014.06.004

12. Frisch MJ (2009) Gaussian 09, Revision E.01, Gaussian, Inc., Wallingford CT, 2013.

13. Shao JX, Cheng XL, Yang XD (2006) The C-NO_2 bond dissociation energies of some nitroaromatic compounds: DFT study. Struct Chem 17: 547-550.

https://doi.org/10.1007/s11224-006-9106-1
14. Zhao Y, Truhlar DG (2008) The M06 suite of density function als for main group thermochemistry, thermochemical kinetics, noncovalent interactions, excited states, and transition elements: two new functionals and systematic testing of four M06-class functionals and 12 other functionals. Theor. Chem. Acc. 120: 215-241.
https://doi.org/10.1007/s00214-007-0310-x
15. Zara Z, Iqbal J, Ayub K, Irfan M, Mahmood A, Khera RA, Eliason B (2017) A comparative study of DFT calculated and experimental UV/Visible spectra for thirty Carboline and carbazole based compounds. J. Mol. Struct. 1149: 282-298.
https://doi.org/10.1016/j.molstruc.2017.07.093
16. Hehre WJ, Ditchfield R, Radom L, Pople JA (1970) Molecular orbital theory of the electronic structure of organic compounds. V. Molecular theory of bond separation. J. Am. Chem. Soc. 92(16): 4796-4801.
https://doi.org/10.1021/ja00719a006
17. Kamlet MJ, Jacobs SJ (1968) Chemistry of detonations. I. A simple method for calculating detonation properties of C-H-N-O explosives. J. Chem. Phys. 48: 23-35.
https://doi.org/10.1063/1.1667908
18. Matito E (2016) An electronic aromaticity index for large rings. Phys. Chem. Chem. Phys. 18: 11839-11846.
https://doi.org/10.1039/C6CP00636A
19. Lu T, Chen FW (2012) Multiwfn: a multifunctional wavefunction analyzer. Comput. Chem. 33: 580-592.
https://doi.org/10.1002/jcc.22885
20. Lu T (2024) A comprehensive electron wavefunction analysis toolbox for chemists, Multiwfn. J. Chem. Phys. 161.
https://doi.org/10.1063/5.0216272
21. Humphrey W, Dalke A, Schulten K (1996) VMD: visual molecular dynamics. J. Mol. Graph. 14(1): 33-38.
https://doi.org/10.1016/0263-7855(96)00018-5
22. VMD for WIN64, version 1.9.4a51 (December 21, 2020)
http://www.ks.uiuc.edu/Research/vmd/
23. Lu T (2020) Molclus program, Version 1.9.5. Bijing Kein Research Center for Natural Science, China. http://www.keinsci.com/research/molclus.html. Accessed 12 Jul 2020
24. Geuenich D, Hess K, Köhler F, Herges R (2005) Anisotropy of the Induced Current Density (ACID), a General Method To Quantify and Visualize Electronic Delocalization. Chem. Rev. 105(10): 3758-3772.
https://doi.org/10.1021/cr0300901

Statements & Declarations

Funding The Doctoral Research Foundation of Huanggang Normal University No. 2042024348; The Doctoral Research Foundation of Huanggang Normal University No. 2042024347; Teaching Research Project of Huanggang Normal University No. 2026CE53.

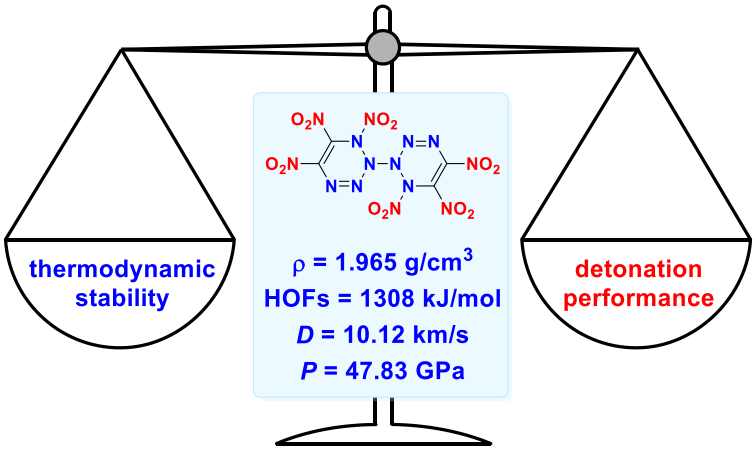
Competing interests The authors have no relevant financial or non-financial interests to disclose.

Author contribution Qian Zhang provided molecule designing scheme and complete theoretical calculation work. Xiaonan He, Hanjie Ni and Jianan Li jointly assisted in completing the data organization. Lanying Xu has completed the image production work. Tao Long offered suggestions and assisted in revising the manuscript. Yan Huang finished writing, checking and editing the manuscript.

Data availability Data is provided within the manuscript or supplementary information files.

Briefs

Tetrazine-based nitrogen-chain frameworks were designed and systematically analyzed *via* DFT calculations, achieving enhanced thermodynamic stability (HOFs 948.8-1954 kJ/mol) and superior detonation performance (detonation velocity 8.926-11.32 km/s, explosion pressure 33.94-59.18 GPa) compared with triazole-based analogues.



Supplementary Files

This is a list of supplementary files associated with this preprint. Click to download.

- JMMsupportinginfomation202609.docx